Design of Subsonic Airfoils for High Lift

Robert H. Liebeck
Douglas Aircraft Company, McDonnell Douglas Corporation, Long Beach, Calif.

Nomenclature

c = airfoil chord
C_L = lift coefficient = $L/\frac{1}{2}\rho V_\infty{}^2 c$
C_{L_u} = upper-surface lift coefficient
C_p = pressure coefficient = $(p-p_\infty)/\frac{1}{2}\rho V_\infty{}^2$
M_∞ = freestream Mach number
p = static pressure
Re_∞ = freestream Reynolds number based on airfoil chord = $V_\infty c/\nu$
s_p = location of leading-edge stagnation point
V_∞ = freestream velocity
v = local velocity on airfoil surface
x = distance along chord line
Γ = circulation about the airfoil
γ = ratio of specific heats
ν = kinematic viscosity
ρ = density
$()_\infty$ = freestream conditions
$()_{t.e.}$ = conditions at the airfoil trailing edge

I. Introduction

WORK on this problem originated as a response to a general question from A.M.O. Smith: "What is the maximum lift which can be obtained from an airfoil, and what is the shape of that airfoil?" Use of the word "maximum" implied that some form of optimization technique must be employed, and consequently the solution of such a problem would be strongly influenced by the various constraints that were imposed. Therefore, in order to classify the problem more specifically, it was required that the airfoil be composed of a single element and that powered lift would not be considered. Two additional constraints were that the flow remain unseparated and subsonic everywhere on the airfoil.

A majority of the airfoil design work to be discussed in this paper is based on the inverse approach; i.e., begin with an airfoil pressure (or velocity) distribution that provides the desired performance, and employ an "inverse" calculation procedure to obtain the corresponding airfoil shape. Three representative studies that use the inverse technique are those of Lighthill,[1] Wortmann,[2] and Goldstein and Mager.[3] Lighthill's work centers primarily on the development of the inverse potential flow calculation method itself, and some sample designs for high lift are presented. On the other hand, Wortmann concentrates on the development of a pressure distribution that provides a low-drag airfoil for sailplane applications. The success of his work is evidenced by the fact that a Wortmann airfoil is used on almost every modern high-performance sailplane. Goldstein and Mager approached the problem of maximizing the circulation of airfoils in cascade, and their basic design philosophy was quite similar to that to be discussed in the present paper. Unfortunately, their results were compromised by the lack of modern potential flow and boundary-layer theories and calculation methods.

A linearized solution to A.M.O. Smith's question was first obtained in Ref. 4, where C_L was expressed in terms of $\int C_p dx$, with the freestream aligned with the x axis. The approach was to optimize the pressure distribution $C_p(x)$ using boundary-layer and potential flow theories together with the calculus of variations, and the second-order inverse airfoil theory of Weber[5] was used to calculate the corresponding shape. It was found that the airfoil designs resulting from this study were highly cambered which suggested that linearized theory was inadequate for a thorough solution of the problem. Reference 4 did, however, demonstrate that such a problem could be formulated and solved.

Guided by the analysis and results of Ref. 4, the nonlinear problem was formulated and solved in Ref. 6. In this case, C_L was expressed in terms of $\oint v ds$, where v is the velocity on the airfoil surface and s is the arc length along the airfoil surface. Using s as the independent variable (as opposed to x, measured along the airfoil chord) is essential for the accurate application of boundary-layer theory. Also, since the true location of the chord line is unknown until the airfoil shape has been calculated, specification of the velocity (or pressure) distribution as a function of s is more precise. In a similar manner to the analysis of Ref. 4, the airfoil velocity distribution $v(s)$ was optimized with several refinements over the earlier work. The exact nonlinear inverse airfoil theory of James[7] was then used to calculate the corresponding airfoil shape. Two of the resulting airfoils were tested in a wind tunnel,[8] and their performance exceeded the theoretical predictions. At the design lift coefficient, the drag was lower than the theoretical value, and the low-drag range of the airfoils was extremely wide. The method of Ref. 6 has been extended to solve a wide variety of airfoil design problems, such as maximizing airfoil thickness for a specified lift coefficient. One of the more promising extensions of this

Robert H. Liebeck received B.S. (1961), M.S. (1962), and Ph.D. (1968) degrees in aeronautical engineering from the University of Illinois. He joined the Douglas Aircraft Company Missile and Space Systems Division in 1961, where he worked primarily in research on supersonic wing theory. In 1967, he transferred to the Douglas Aircraft Company as a senior scientist in the Aerodynamics Research Group working on the development of advanced airfoils. Two patents are pending on the resulting airfoil designs. Since 1974, he has been working in the Aerodynamic Configuration Design Group on advanced design military aircraft, as well as continuing his research on airfoils. He has also been active as a consultant on a variety of projects which include windmill design and the aerodynamic design of racing cars. Dr. Liebeck has taught in the Graduate Schools at the University of California at Irvine and California State University at Long Beach. Currently, he is an Adjunct Professor of Aerospace Engineering at the University of Southern California teaching airplane design. He is an Associate Fellow of the AIAA.

Presented as Paper 76-406 at the AIAA 9th Fluid and Plasma Dynamics Conference, San Diego, Calif., July 14-16, 1976; submitted July 13, 1976; revision received April 24, 1978.
Index category: Aerodynamics.

work involves the design of optimized airfoils for operation in the compressible flow regime.

The problem of designing a maximum lift airfoil has recently received the attention of several researchers, and the following are some examples. A theoretical approach similar to that of Ref. 6 was used by Ormsbee and Chen,[9] and an airfoil designed using their method was subsequently tested in a wind tunnel.[10] The results show a drag rise at higher lift coefficients which appears to be a consequence of their formulation of the trailing-edge condition; however, the overall performance of this airfoil substantiates the viability of the basic approach. Another similar study was conducted by Pick and Lien[11] where, in addition to designing for maximum lift, it was required that the resulting airfoil have a specified thickness distribution. Thin airfoil theory was used to generate their initial solutions, which were then refined using the exact nonlinear method of James.[7] The resulting airfoil was tested in a wind tunnel, with good results. Strand[12] has developed a modification to the inverse method of Arlinger[13] which he uses to derive the airfoil designed by Pick and Lien as a test case, along with some similar airfoil designs. At this writing, it is not known if any of Strand's airfoils have been tested. Finally, Wortmann[14] has approached the problem of maximum lift airfoil design on the basis of obtaining the minimum sink rate for a sailplane. His analytical approach is entirely different from that employed in the preceding references; however, the resulting airfoils have shown good performance in wind-tunnel tests. A comparison of the wind-tunnel results of Ref. 10, 11, and 14 with those of Ref. 8 is given later in this paper.

If the restriction to a single element is removed from the maximum lift problem, a considerable increase in the attainable lift becomes possible. The method of Ref. 6 has been extended to study the optimization of multielement airfoils, and the preliminary designs obtained thus far appear promising. The analysis suggests the optimum number of elements and their respective chord lengths for a given Reynolds number and Mach number, together with the specification of the pressure distribution for each of the elements. Progress in this work has been limited by the lack of a viable inverse solution technique for multielement design. However, using a combination inverse-direct technique, the author has developed some two-element high-lift airfoil designs that have been successful in application as race car wings. A very thorough discussion of the general multielement design problem is given by Smith.[15]

This paper describes some of the development and testing of optimized airfoil designs at Douglas over the past 10 years. Included are example solutions and wind-tunnel test results, together with the results from some applications. At several points, recommendations for further and/or more detailed studies are offered.

II. Single-Element Airfoil Development

Reference 8 describes the solution of the single-element high-lift airfoil design problem, together with an experimental verification of the resulting airfoil performance. A brief outline is presented here in order to provide a background for the work described in this paper.

A. Formulation of "Optimized Velocity Distribution"

In order to study the problem of maximizing the lift of a single-element airfoil, some definitions and contraints must first be established. The basic approach is to optimize a velocity (or pressure) distribution that maximizes the lift, and then compute the corresponding airfoil shape. This velocity distribution must satisfy three criteria: 1) the flow remains subsonic and unseparated everywhere; 2) the corresponding airfoil shape is physically possible; and 3) maximum C_L is obtained. A variational problem can now be set where an extremum of C_L is sought subject to the constraints of criteria 1 and 2.

The general form of an airfoil velocity distribution is shown in Fig. 1, where s, the arc length along the airfoil surface, is chosen as the independent variable. Since the only known point of an airfoil yet to be designed is the trailing edge, this is chosen as the origin, with s proceeding clockwise around the airfoil surface to the upper-surface trailing edge. The total perimeter of airfoil is normalized to unity which implies a nonunit chord.

The lift coefficient, expressed in terms of the circulation Γ about the airfoil, is given by

$$C_L = \frac{L}{\frac{1}{2}V_\infty{}^2 c} = \frac{2\Gamma}{V_\infty c} = 2\oint \frac{v(s)}{V_\infty}\frac{ds}{c}$$

where $v(s)$ is the velocity distribution on the surface of the airfoil. Criterion 1 constrains $v(s)$ in terms of boundary-layer separation, and criterion 2 in terms of potential flow requires that $v(s)$ must have a leading-edge stagnation point $s=s_p$, and it must also satisfy the Kutta condition at the trailing edge.

Since $v(s)\leq 0$ everywhere on the lower surface, C_L will be maximized by keeping $v(s)$ as close to stagnation as possible. Alternatively, $v(s)\geq 0$ on the upper surface implies that $v(s)$ should be maximized there to obtain a maximum for C_L. The lower surface $v(s)$ is less likely to be affected by the restrictions of criterion 1, and therefore it is left unspecified at this stage of the analysis. The following section briefly describes the application of boundary-layer theory and the calculus of variations to the determination of the upper-surface velocity distribution $v(s)$, which maximizes C_L.

Referring again to Fig. 1, the form of the upper-surface velocity distributions calls for an acceleration from stagnation up to some peak velocity, followed by a deceleration (pressure recovery) back to $v_{t.e.}/V_\infty < 1$. It is desired to maximize the area under the v/V_∞ versus s curve subject to the constraint that the boundary layer does not separate. Stratford[16] has developed an analytical method that provides a pressure recovery (deceleration) distribution which continuously avoids separation by a constant specified margin. This form of pressure recovery in principle recovers a given ΔC_P in the shortest possible distance, or it can be interpreted as recovery of the maximum ΔC_P in a given distance. Therefore, the Stratford imminent separation pressure recovery distribution appears to be ideal for maximizing C_{L_u} as given by

$$C_L = C_{L_\ell} + C_{L_u} + \frac{2}{c}\int_0^{s_p} v(s)\,ds + \int_{s_p}^{1} v(s)\,ds$$

Stratford[17] has experimentally checked a flow using his pressure recovery distribution and found that it did not separate and exhibited "a good margin of stability."

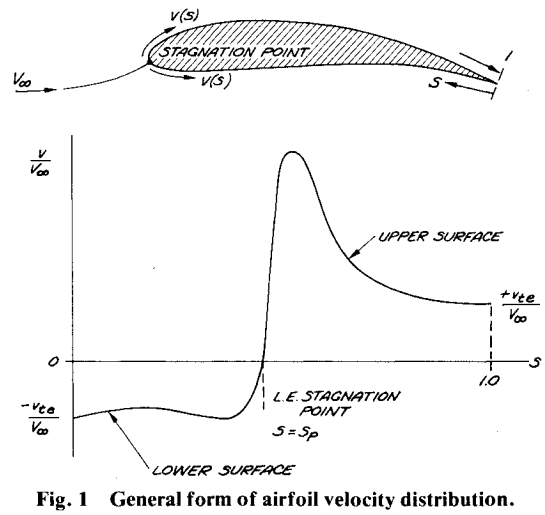

Fig. 1 General form of airfoil velocity distribution.

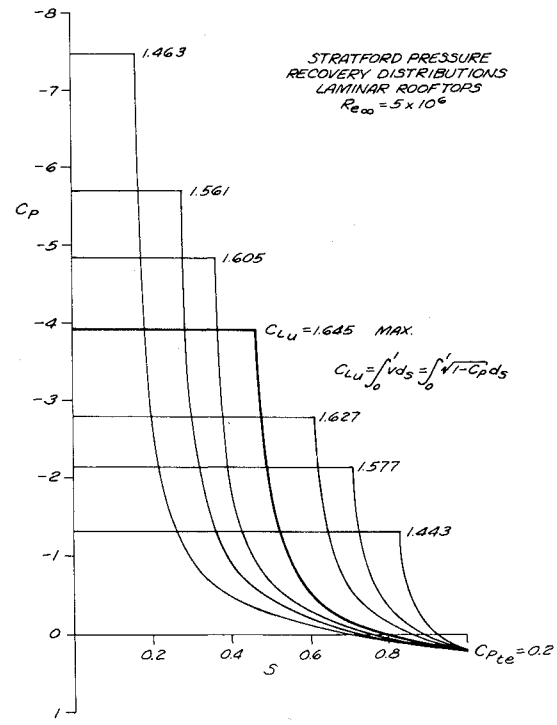

Fig. 2 Family of optimized upper-surface pressure distributions.

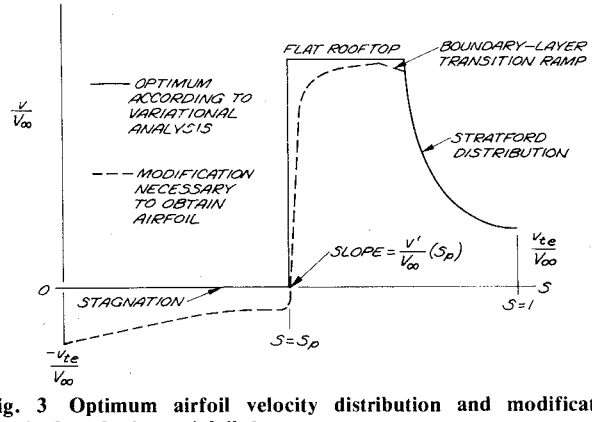

Fig. 3 Optimum airfoil velocity distribution and modification required to obtain an airfoil shape.

Applying the calculus of variations yields the basic solution that a pressure distribution given by a flat rooftop followed by a Stratford recovery distribution maximizes C_{L_u} for an arbitrary specified location of the transition point on the rooftop. There exists an infinite family of such flat rooftop distributions for a fixed set of the parameters $v_{t.e.}/V_\infty$ and Re_∞, and the variational solution also specifies the particular member of the family which maximizes C_{L_u} (Fig. 2). It should be noted that, for a fixed set of the parameters $v_{t.e.}/V_\infty$ and Re_∞, the resulting optimum velocity distribution for a laminar rooftop will have a longer and higher rooftop region than for a turbulent rooftop.

The preceding analysis has indicated that C_L will be maximized by a velocity distribution of the form shown by the solid line in Fig. 3. This distribution is made up of $v/V_\infty = 0$ over the entire lower surface and $v(s)/V_\infty$ given by a flat rooftop plus Stratford distribution on the upper surface. Although this distribution is satisfactory in terms of the boundary-layer requirements of criterion 1, it will not satisfy criterion 2 and provide an airfoil shape. The discontinuities implied at the leading and trailing edges and the fact that true stagnation can occur only at a single point prevent a meaningful potential flow solution.

Therefore, the velocity distribution has been modified as shown by the broken line in Fig. 3. The slope $v'(s_p)$ affects the leading-edge radius and thickness of the resulting airfoil shape, and the remaining portion of the upper-surface rooftop region is shaped to allow for operation at angles of attack above the design value. A boundary-layer transition ramp has been located at the rooftop peak for those cases where the rooftop is laminar and also to ease a turbulent boundary layer's introduction to the severe initial Stratford gradient. The proper shaping of the transition region becomes extremely critical at Reynolds numbers below 10^6, and this will be discussed later.

For the maximum lift problem, the lower-surface distribution is modified according to two general constraints: 1) the velocity remains as low as possible in order to obtain maximum lift, and 2) the flow continuously accelerates in the interest of minimizing the drag. Near the stagnation point, the distribution is shaped to provide good off-design performance at lower angles of attack.

A very important parameter is the trailing-edge velocity ratio $v_{t.e.}/V_\infty$. The choice of a high value for $v_{t.e.}/V_\infty$ is very desirable from the standpoint of increasing the upper-surface lift C_{L_u}. (For example, a 10% increase in $v_{t.e.}/V_\infty$ may increase C_{L_u} as much as 15%.) However, $v_{t.e.}/V_\infty$ is severely limited by the consideration of obtaining a proper trailing-edge geometry. According to potential flow theory, the value of $v_{t.e.}/V_\infty$ at the trailing edge of a cusped airfoil is always less than one. For a given family of airfoils of varying thickness, reducing the thickness results in a corresponding increase in the value of $v_{t.e.}/V_\infty$. In the case of a symmetric airfoil at zero angle of attack, $v_{t.e.}/V_\infty$ becomes unity as the thickness goes to zero which corresponds to a flat plate. This is the only case where $v_{t.e.}/V_\infty = 1$. Any thickness, camber, or lift requires that $v_{t.e.}/V_\infty < 1$. It is possible in potential flow to have $v/V_\infty > 1$ just upstream of the trailing edge; however, this implies a large trailing-edge angle. This will encourage the real flow to separate upstream of the trailing edge which will result in an increase in drag and a loss of lift due to a modified Kutta condition. It has been found that acceptable values of $v_{t.e.}/V_\infty$ lie between 0.80, and 0.95, depending on the airfoil thickness and design lift coefficient.

In summary, the airfoil velocity distribution has been optimized, satisfying boundary-layer theory, and then modified in the interest of satisfying potential flow theory. The free parameters include the slope $v'(s)/V_\infty$ at $s = s_p$, the value of s_p, and $v_{t.e.}/V_\infty$, along with the shape of the lower-surface distribution and the upper- and lower-surface acceleration regions. The velocity distribution as modified in the preceding discussion can no longer be called optimum in a purely mathematical sense. For the lack of a better phrase, they will be referred to as "optimum velocity distributions" with the understanding that this qualification exists.

B. Inverse Airfoil Solution

Once a desired optimum airfoil velocity distribution has been developed, it remains to determine the corresponding airfoil's shape. James[7] has developed a powerful inverse airfoil design program that provides essentially exact solutions for the incompressible airfoil design problem. A prescribed velocity distribution will not necessarily conform to a closed airfoil with the proper flow conditions at infinity. Therefore, some compromise to the input distribution is inevitable, and the James program returns as output a shape and velocity that are an exact solution pair, where the velocity is changed to meet the closure and infinity conditions by preserving the input details while modifying certain of the overall characteristics. By comparing the input and resulting modified (output) velocity distribution, the input distribution is easily adjusted (by varying $v_{t.e.}/V_\infty$, s_p, the level of the lower surface velcoity distribution, etc.), so that agreement between the input and output distributions is obtained.

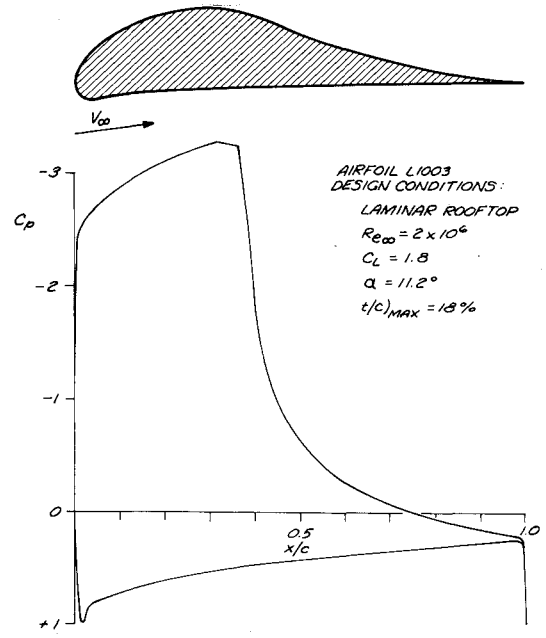

Fig. 4 Airfoil L1003 and its pressure distribution at the design angle of attack.

C. Example Solutions for the Maximum Lift Problem and Their Experimental Evaluation

Initially, two "prototype" airfoils were designed for testing in the McDonnell Douglas low-speed wind tunnel in St. Louis: airfoil L1003 (shown in Fig. 4), which assumed a laminar boundary layer over the rooftop region, and airfoil L1004 (not shown), which assumed the boundary layer to be turbulent over the entire airfoil surface. A thorough description of the design and testing of these airfoils is given in Ref. 8. More recently, three airfoils designed for Reynolds numbers of less than 0.50×10^6 were tested in the Douglas Long Beach wind tunnel, and the results are given in Ref. 18. The best of the three airfoils (airfoil LA2566) is shown in Fig. 5. Aluminum pressure instrumented models were used for all of the tests, and the drag was obtained using wake pressure data.

Airfoil L1003 was designed for a Reynolds number of 2×10^6 with the requirement that laminar flow be maintained over the entire rooftop region, and premature transition should, in principle, render the boundary layer incapable of negotiating the pressure recovery region. When the design Reynolds number is on the order of 1.0×10^6 and below, the problem shifts from prolonging laminar flow to that of obtaining proper transition to a turbulent boundary layer. (Depending on airfoil surface quality and the freestream turbulence level, it is possible to experience such problems at Reynolds numbers as high as 5×10^6.) Three test airfoils were designed for a Reynolds number of 0.25×10^6, each with a slightly different design philosophy for the shaping of the rooftop region. All three were designed with relatively large thickness for high-aspect-ratio applications. Airfoil LA2563 (not shown) was designed using the maximum lift upper-surface velocity distribution and a relatively short transition ramp. Because of the low design Reynolds number, this resulted in a very short rooftop length of approximately 25% chord. In the interest of obtaining a higher value for the local Reynolds number at the rooftop peak to help promote transition, airfoil LA2564 (not shown) was designed which had a longer rooftop of approximately 35% chord and a short transition ramp. (It turns out that, even though the rooftop level is reduced when the length is extended as shown in Fig. 2, the local Reynolds number is increased.) Finally, airfoil LA2566 (Fig. 5) was designed with a long transition ramp; otherwise, it is identical to airfoil LA2564.

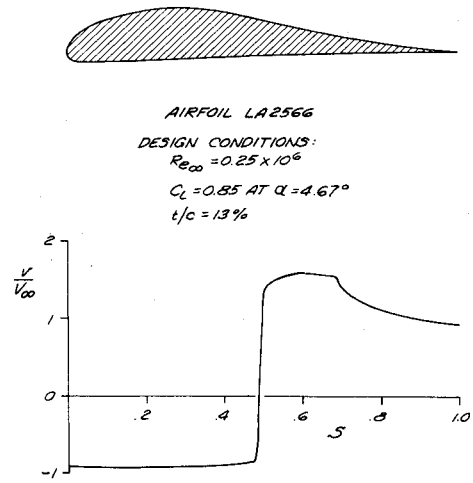

Fig. 5 Airfoil LA2566 and its velocity distribution at the design angle of attack.

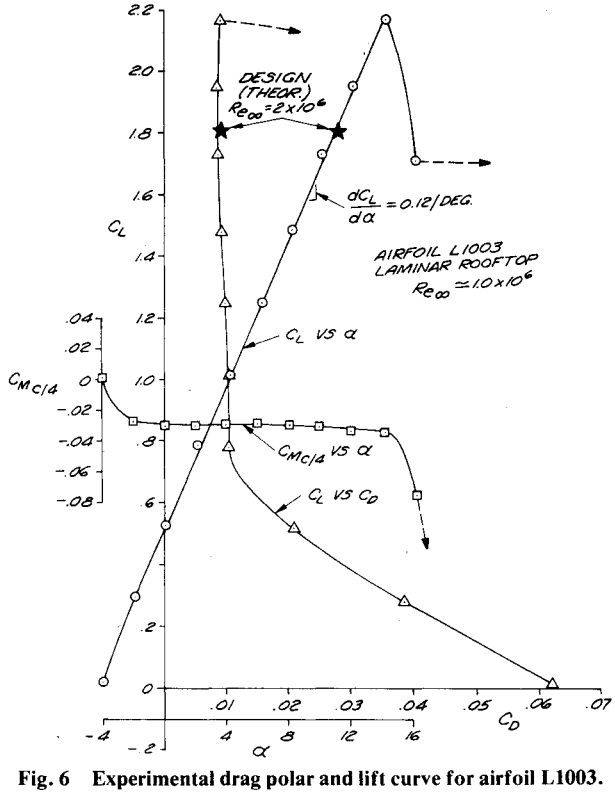

Fig. 6 Experimental drag polar and lift curve for airfoil L1003.

The performance of all of the test airfoils (L1003, L1004, LA2563, LA2564, and LA2566) was checked using the Douglas MADAAM computer program,[19] which combines the potential flow solution of Ref. 20 with the boundary-layer calculation of Ref. 21. In all cases, the flow was predicted to remain attached not only at the design condition but also over a significant angle-of-attack range. This implied some conservatism in the Stratford recovery distribution. Moving the theoretical transition point forward of the rooftop peak on the laminar rooftop airfoils eventually caused separation to be predicted, whereas airfoil L1004, designed with a turbulent rooftop, was unaffected in terms of separation. In the case of airfoils LA2563, LA2564, and LA2566, a short laminar separation bubble with turbulent reattachment was predicted at the start of the recovery region at the design Reynolds number of 0.25×10^6 for all three airfoils.

The results of the wind-tunnel test of airfoil L1003 are shown in Fig. 6. It is necessary to conduct most of the testing

of airfoil L1003 (laminar rooftop) at $Re_\infty 1.0\times10^6$ because freestream turbulence in the St. Louis tunnel test section caused premature transition on the rooftop region when the tunnel was operated at higher Reynolds numbers. In fact, the addition of a transition strip on the rooftop region near the leading edge reduced the airfoil's $C_{L_{max}}$ to about 1.0. This was expected, since this airfoil was optimized assuming a laminar rooftop. If it had not stalled early, the implication would be that a proper optimization had not been achieved. Airfoil L1004, designed assuming a turbulent boundary layer over the entire rooftop region, was also tested amd reached design C_L even when a transition strip was located at the leading edge. It behaved very well at a Reynolds number from 1.0×10^6 to 3.0×10^6, which were the limits of the tunnel capability.

The mechanism of the stalling of airfoils L1003 and L1004 was observed using yarn tufts located on the upper-surface pressure recovery region. Both airfoils exhibited the same behavior in that the flow remained completely attached until the stalling angle was reached, at which point the entire recovery region separated instantaneously. Reducing the angle of attack less than ½ deg resulted in an instantaneous and complete reattachment, indicating almost a total lack of hysteresis effect on stall recovery. The presence of yarn tufts on the recovery region had no apparent effect on the airfoil's performance in terms of increased drag or reduced $C_{L_{max}}$. Throughout the testing, the flow on the recovery region appeared extremely stable up to the point where stall occurred.

The three low Reynolds number airfoils were tested at Reynolds numbers of 0.5×10^6 and 0.25×10^6 in the Long Beach tunnel. Airfoil LA2563 required a transition strip at the rooftop in order to remain attached at the design angle of attack at 0.5×10^6, and 0.35×10^6 was the lowest Reynolds number at which the airfoil operated properly. Airfoil LA2564 remained attached without a transition strip at 0.50×10^6 but required a strip at 0.25×10^6. From an operational point of view, neither of these airfoils could be regarded as acceptable below 0.50×10^6.

Airfoil LA2566 performed quite well without a transition strip at 0.25×10^6, and the addition of a strip midway along the transition ramp only served to reduce the drag slightly at the lower lift coefficients, with $C_{L_{max}}$ remaining unchanged. Flow visualization using napthalene and a comparison of the chordwise pressure distributions revealed that a very short (2% chord) laminar separation bubble existed at the rooftop peak, and this was removed by the transition strip. Evidently, although the $C_{L_{max}}$ and the basic pressure distribution are unaffected by the pressure of the small bubble, it does serve to increase the boundary-layer thickness and thus increase the drag. The drag polars and lift curves for $Re_\infty = 0.25\times10^6$ and 0.50×10^6 are shown in Fig. 7.

It should be noted that the turbulence level of the Long Beach tunnel was extremely low, and the model quality was very smooth for these tests. An NACA 4415 airfoil that was tested as a baseline showed transition considerably further aft than predicted by theory. Consequently, it is felt that airfoil LA2566 may perform quite well without a transition strip in most applications. Natural transition without a laminar bubble is not guaranteed, but it is likely to occur. On the basis of the results obtained thus far, it appears that a long rooftop and long transition ramp are required; however, much more testing needs to be done in this flow regime.

The form of the pressure distribution of airfoil LA2566 may have an additional virtue in terms of low Reynolds number operation. An airfoil such as an NACA 4415 has a more or less constant adverse gradient extending from the pressure peak near the leading edge all the way to the trailing edge. The boundary layer sees the same adverse gradient continuously, and the transition point location becomes a strong function of freestream turbulence and surface roughness. Changes in the location of transition, in turn, have a significant effect on drag and possibly $C_{L_{max}}$. Alternatively,

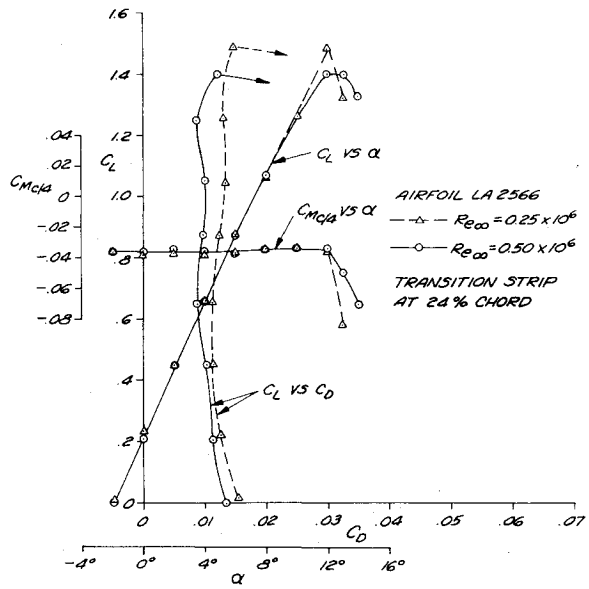

Fig. 7 Experimental drag polars and lift curves for airfoil LA2566.

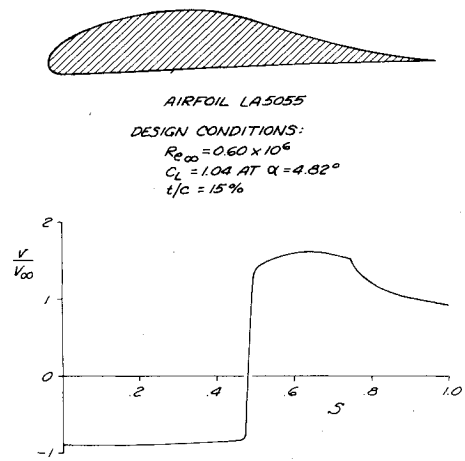

Fig. 8 Airfoil LA5055 and its velcoity distribution at the design angle of attack.

airfoils like LA2566 should not be as sensitive to turbulence level and surface roughness because the rooftop has a favorable gradient, and it is unlikely that premature transition could occur there at low Reynolds numbers. In fact, it is possible that a moderate level of turbulence and/or roughness would improve the performance of such airfoils, as mentioned previously.

The presence of a laminar bubble or a transition strip did not appear to affect the stability of the flow on the recovery region, which suggests that the Stratford distribution may be somewhat conservative, particularly at low Reynolds numbers. If this is true, narrowing the margin of conservatism could improve the performance of the airfoil. Increasing the design Reynolds number to between 0.50×10^6 and 1.0×10^6 will result in a Stratford distribution whose "margin" from separation is reduced when the airfoil is operated at 0.25×10^6. In addition, the rooftop length and level will be increased, and this will provide a higher local Reynolds number at the rooftop peak which, in turn, reduces probability of a laminar bubble forming. As an example, a "second-generation" low Reynolds number airfoil has been designed at $Re_\infty = 0.25\times10^6$, and the result, airfoil LA5055, is shown in Fig. 8. This should only be regarded as a next possible step in an area of airfoil design which has received relatively little attention.

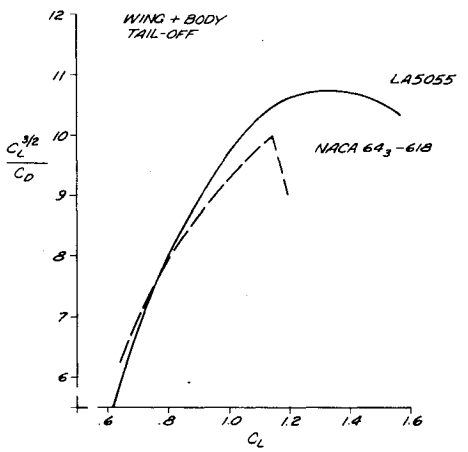

Fig. 9 Experimental results for $C_L^{3/2}/C_D$ for two wings as tested by the Navy in the DTNSRDC 8- × 10-ft subsonic wind tunnel.

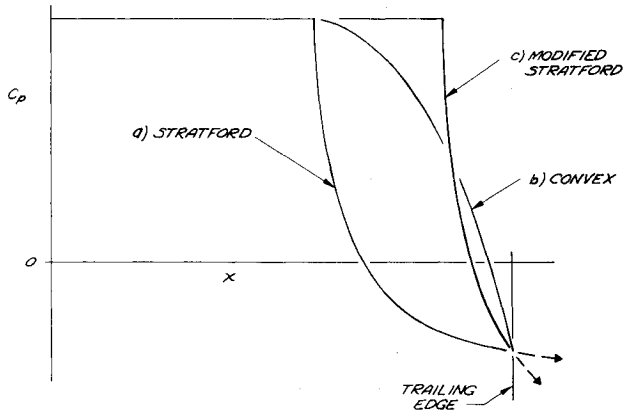

Fig. 10 Comparison of pressure recovery distributions.

A wing using airfoil LA5055 was tested by the Navy in the 8- × 10-ft subsonic wind tunnel at the David Taylor Naval Ship Research and Development Center. The intended application was a long-endurance patrol airplane, and hence a maximum of the parameter $C_L^{3/2}/C_D$ was sought. Two wing-body combinations were tested: one using the LA5055 airfoil, and the other using an NACA 64_3-618 airfoil. Both wings were of identical planform, with an aspect ratio of 12 and no sweep. Figure 9 gives the resulting variation of $C_L^{3/2}/C_D$ with C_L for the two wings. In addition, the NACA 64_3-618 wing began to separate at $C_L = 1.07$ and had a $C_{L_{max}}$ of 1.22, whereas the LA5055 wing exhibited no separation until $C_{L_{max}}$ of 1.58 was reached. It should be noted that a significant portion of the drag above $C_L = 1.0$ was probably due to the fuselage being at a relatively high angle of attack ($\alpha \approx 6$ deg at $C_L = 1.0$). A thorough description of this test is given in Ref. 22.

D. Comments on the Stratford Distribution

At this point, it will be useful to discuss the Stratford recovery distribution as it has been found to apply to the airfoil design problem. Considered in the form shown in Fig. 3 for the upper-surface velocity distribution, it provides a unique path in the v-s plane from the rooftop peak to the trailing edge at $v_{t.e.}$. That is, the Stratford distribution is the only way to get from the rooftop peak to the trailing edge without separation. Obviously a steeper initial portion of the curve will cause separation. On the other hand, if a milder gradient is used, separation will not occur in that region. However, a much steeper gradient will eventually be required in order to reach the trailing-edge velocity $v_{t.e.}$, and this will cause separation somewhere along the aft portion of the recovery region.

Instead of thinking of the Stratford distribution as imminently separating everywhere, it can be interpreted as a recovery distribution that avoids separation by a constant "margin" along its entire length. The boundary layer may be considered as being no more ready to separate at the trailing edge than it is near the beginning of the recovery region. Similarly, the stalling behavior described in the previous section indicates that, when said margin is used up, separation occurs simultaneously everywhere on the recovery region. In principle, a Stratford recovery region extends to downstream infinity with a continuously decreasing gradient, as shown by the broken lines in Fig. 10. This is an oversimplification, and it is only intended to describe the character of a Stratford recovery distribution.

Figure 10 shows a comparison of a Stratford distribution, a modified Stratford distribution, and a convex pressure recovery distribution. All three distributions have been derived on the basis of proceeding as far aft as possible at the specified rooftop C_p level and then recovering to a specified trailing-edge value of C_p without separation. For relatively low rooftop levels ($C_p \approx -1.0$), it can be shown that the effective lift $\int C_p dx$ of the convex distribution can be equivalent to that of the Stratford distribution. As the rooftop level reaches $C_p \approx -2.0$ and higher, the Stratford recovery becomes clearly superior in terms of upper-surface lift. Nevertheless, the convex distribution at the lower rooftop levels as sketched in Fig. 10 appears to contradict the claims about the unique path of the Stratford distribution until the following distinction is made.

The convex distribution of Fig. 10 has been derived using the Cebeci turbulent boundary-layer program[23] such that separation is predicted at the trailing edge. An increase in airfoil angle of attack would cause the separation point to move forward from the trailing edge, and this would result in the characteristic round-over of the lift curve and increase in drag at higher lift coefficients.

In the case of an airfoil with a Stratford recovery distribution, an increase in the angle of attack simply reduces the margin from separation along the entire recovery region. There is no round-over in the lift curve and no significant increase in drag, and this has been substantiated by the test results described in the previous section and in Ref. 8. If the angle of attack is increased to the point where the margin vanishes, the entire recovery region separates simultaneously, as observed in the wind-tunnel tests.

The term "margin" as used in the preceding discussion is difficult to define precisely using conventional boundary-layer parameters, and it has been used here to describe heuristically the behavior of the Stratford recovery distribution. It is controlled by an empirically derived constant multiplier of the Reynolds number term in the basic equations of Stratford, and the value used in the design of the airfoils discussed in this paper is that recommended by Stratford. Specifying a higher design Reynolds number in effect reduces the margin when the airfoil is operated at a lower Reynolds number. The modified Stratford distribution shown in Fig. 10 is a sample result of reducing the margin.

At this writing, it is not clear what the ideal margin should be, and it is likely to vary with the application. It would appear that a careful experimental study of the boundary layer in a Stratford recovery distribution is in order. Also, additional forms of pressure recovery distributions should be studied both theoretically and experimentally. The powerful theoretical method of Cebeci et al.[23] which calculates the pressure distribution required to produce a specified skin friction distribution should be very useful in such work.

III. Extension of Single-Element Design Method

Some extensions and refinements of the method are now discussed which include the design for more specific constraints and the initial development of the solution for compressible flow.

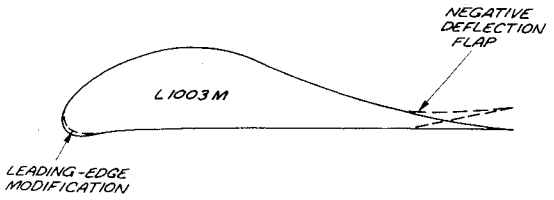

Fig. 11 Modification of airfoil L1003 to obtain L1003M.

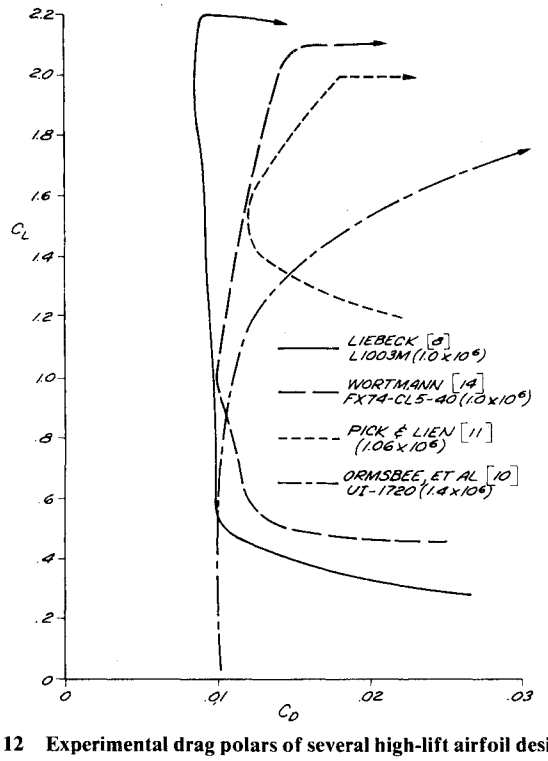

Fig. 12 Experimental drag polars of several high-lift airfoil designs.

A. Modification for Increased Low-Drag Range

Airfoil L1003 exhibited a relatively wide C_L range (0.7 to 2.2) over which the drag remained low, as shown in the wind-tunnel results of Fig. 5. Below $C_L = 0.7$, a pressure spike on the lower surface of the airfoil causes a laminar separation bubble to form which, in turn, results in a large increase in drag. By slightly modifying the leading edge on the lower surface as shown in Fig. 11, the low-drag range has been extended down to $C_L = 0.4$, and adding a 17% chord flap with negative deflection drops the low-drag range to $C_L = 0$.

The resulting drag polar airfoil L1003 is shown in Fig. 12, along with the polars of several airfoils with similar design goals. Wortman's airfoil FX74-CL5-40 was designed for high lift in order to obtain minimum sinking speed for a sailplane,[14] and the test results were obtained in his low Reynolds number wind tunnel at the University of Stuttgart. Airfoil UI-1720 was developed by Ormsbee et al. at the University of Illinois[10] using a method similar to that of Ref. 6 and tested in the University of Illinois low-speed wind tunnel. The airfoil developed by Pick and Lien[11] for long endurance uses a design philosophy similar to that of Ref. 6 but additional constraints on the thickness distribution, and the testing was conducted in the Boeing two-dimensional research tunnel.

The comparisons shown in Fig. 12 should be judged somewhat cautiously. Each airfoil was tested in a different wind-tunnel facility and in some cases at different Reynolds numbers. Typically, an increase in Reynolds number will reduce the drag and increase the $C_{L_{max}}$ of these airfoils; however, factors such as tunnel turbulence and flow quality, model quality, and testing technique are, of course, fundamental to the comparison of such results. The results shown in Fig. 12 do indicate that there has been good progress in the design of airfoils for low drag at high-lift coefficients.

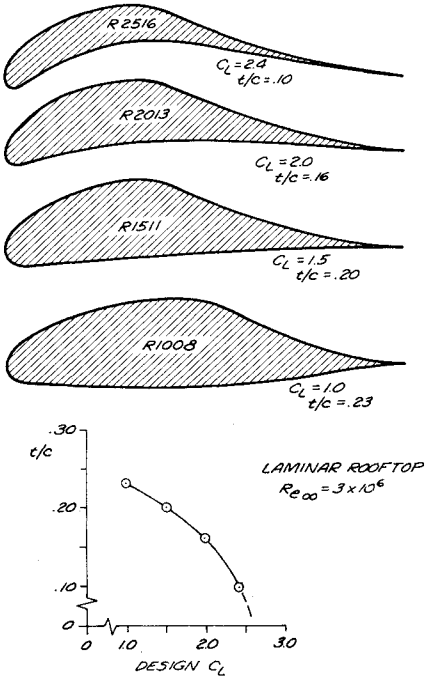

Fig. 13 Effect of design C_L on airfoil thickness.

B. Design for Other Constraints

The variational analysis mentioned in the theoretical development of Sec. II.A showed that a particular flat rooftop plus Stratford recovery velocity distribution provides maximum upper-surface lift. However, other members of the infinite family of pressure distributions shown in Fig. 2 are also useful. A velocity distribution whose rooftop level is less than that of the maximum lift distribution may be interpreted as providing the maximum lift subject to the constraint that the velocity does not exceed some specified value. A similar interpretation is that such a distribution carries the rooftop velocity level as far aft on the airfoil as possible, and this has virtue in terms of obtaining low drag. Therefore, the rooftop level (or length) is an additional parameter that is available for airfoil design. It is unlikely that rooftop levels above the maximum lift value would be very useful.

Another key parameter in the specification of the upper-surface velocity distribution is the assumed location of the transition point. It is essential that laminar flow be maintained at least as far as the specified location of the transition point. If transition moves forward of this location, the airfoil may stall prematurely, possibly before reaching its design lift coefficient. This was demonstrated in the testing of airfoils L1003 and L1004 described in Sec. II.C. Alternatively, if laminar flow extends beyond the specified transition location, the airfoil's performance should improve over the design condition in terms of reduced drag and a possible increase in $C_{L_{max}}$. At Reynolds numbers below 10^6, it is possible that there will be difficulty in obtaining natural transition, as was shown in the testing of airfoil LA2566; however, the present discussion will be concerned with Reynolds numbers on the order of 3×10^6 and above where avoiding early transition is the problem, particularly when a smooth airfoil surface cannot necessarily be assumed.

The following example designs are intended to demonstrate the range of airfoil designs which the additional parameters are capable of providing. For a given set of design conditions (e.g., Reynolds number, C_L, transition point location), each of the airfoils has been designed to be as thick as possible.

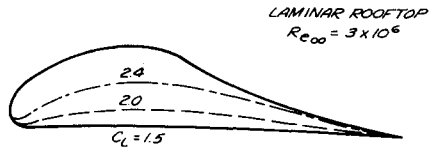

Fig. 14 Comparison of airfoil geometries for varying design C_L.

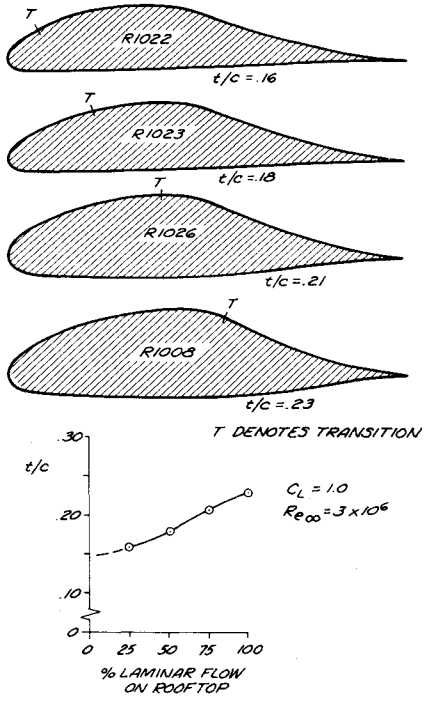

Fig. 15 Effect of transition location on airfoil thickness, $C_L = 1.0$, $Re_\infty = 3 \times 10^6$.

The effect on airfoil thickness of varying the design lift coefficient is given in Fig. 13. Laminar flow over the entire rooftop region was assumed for the four airfoils shown in the figure. These results suggest that a practical upper bound for the design lift coefficient is on the order of 2.0 for a Reynolds number of 3×10^6, particularly since these airfoils have been designed assuming the best possible condition for the boundary layer on the rooftop region (i.e., 100% laminar). The airfoil designed for $C_L = 2.4$ is probably too thin for a practical wing design, and the C_L range over which it would provide low drag would be quite narrow. Figure 14 shows the top three airfoils of Fig. 13 plotted on the same chord line. The upper-surface shapes of the airfoils are almost identical, which is a consequence of the upper-surface velocity distribution being virtually the same for all three airfoils. Thickness serves to decamber the airfoil and hence reduces its lift.

The effect of boundary-layer transition point location on the resulting airfoil thickness for a fixed design C_L of 1.0 and 1.5 is shown in Figs. 15 and 16. The airfoil thickness increases as the extent of laminar flow is increased, and this effect becomes more pronounced as the design lift coefficient is increased. These results demonstrate that, in addition to the reduction in drag provided by laminar flow, a very significant increase in airfoil thickness can be obtained.

Figure 16 shows the effect of reducing the peak velocity (and hence extending the rooftop length) on the airfoil thickness at a fixed C_L of 1.5. Reducing the maximum velocity will increase the Mach number at which compressibility effects begin to degrade the airfoil's performance, and Fig. 17 indicates that there is very little loss in thickness when v_{max}/V_∞ is reduced from 2.0 to 1.8. In fact, airfoil R1506 has a thickness distribution that may be more ap-

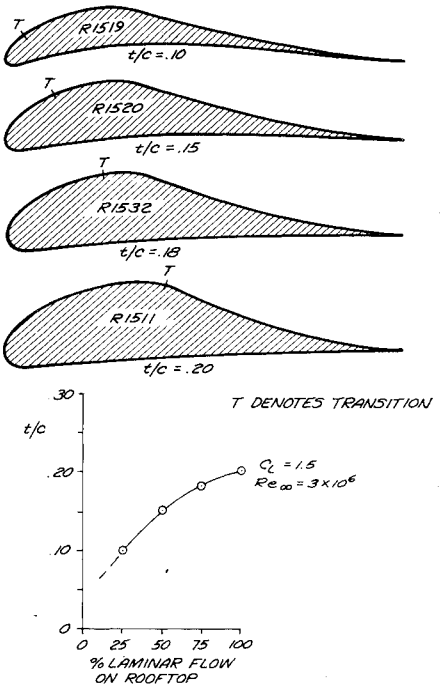

Fig. 16 Effect of transition location on airfoil thickness, $C_L = 1.5$, $Re_\infty = 3 \times 10^6$.

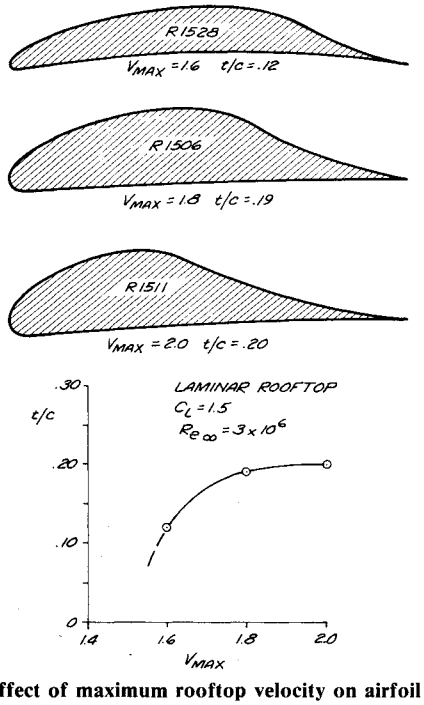

Fig. 17 Effect of maximum rooftop velocity on airfoil thickness at constant $C_L = 1.5$.

pealing from a structural point of view. However, the extended rooftop of this airfoil, together with its reduced leading-edge radius, will tend to narrow the range of lift coefficients over which the drag remains low, and the $C_{L_{max}}$ will probably be less than that of airfoil R1511. The comparisons become more vivid when airfoil R1528 with $v_{max}/V_\infty = 1.6$ is considered. A detailed discussion of the design tradeoffs and options of the type shown in Figs. 13-17 is given in Ref. 24.

C. Design for Compressible Flow

The airfoil designs discussed thus far have been developed assuming incompressible flow. If the flat rooftop plus

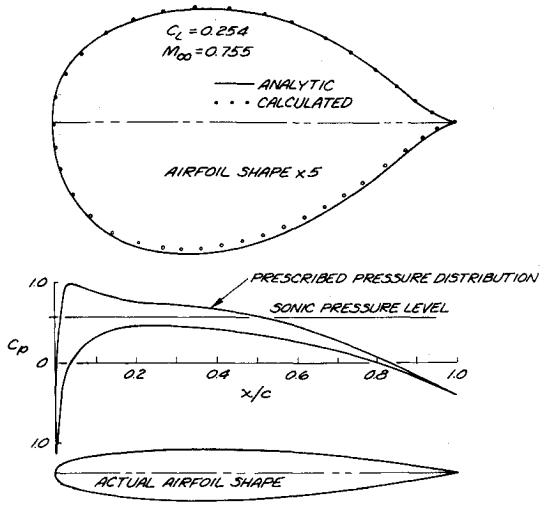

Fig. 18 Comparison of James approximate design method with the exact solution of a lifting supercritical Nieuwland airfoil.

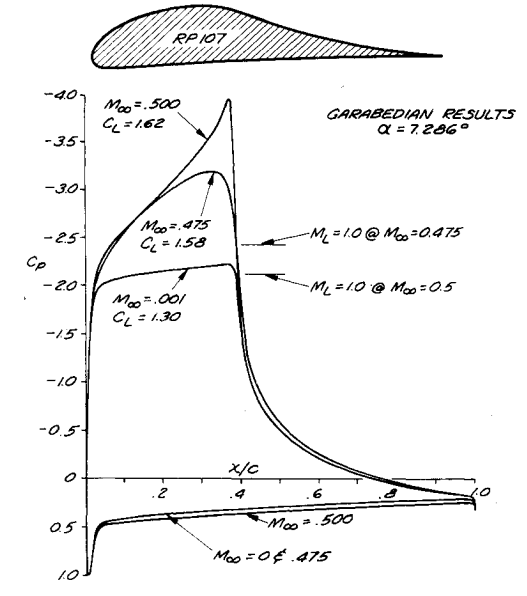

Fig. 19 Airfoil RP107 and its pressure distributions at various Mach numbers as calculated by the method of Ref. 26.

Stratford recovery velocity distribution is viewed from the standpoint of providing maximum lift for a specified maximum rooftop velocity level, it appears that such a distribution could be useful in the design of an airfoil for operation in a subcritical compressible flow.

Stratford's theory[16] was developed for incompressible flow, and therefore the application to compressible flow requires some consideration. For the preliminary studies conducted thus far, a very simple approximation has been used with good results, namely, the velocity distribution is defined such that the compressible pressure distribution corresponds to that of the incompressible Stratford recovery distribution. A possible justification for this relates to the fact that the portion of the boundary layer closest to the airfoil surface is the most critical in terms of separation, and the flow there is within the incompressible range as long as the flow at the edge of the boundary layer remains subcritical. Thus, if the pressure distribution is prescribed according to the Stratford theory, the inner portion of the boundary layer should behave properly. Trial distributions so derived have been checked using the Cebeci compressible turbulent boundary-layer program,[21] and separation is not predicted.

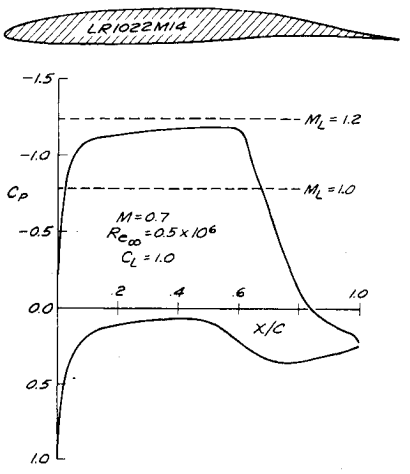

Fig. 20 Airfoil LR1022M14 and its pressure distribution at the design condition.

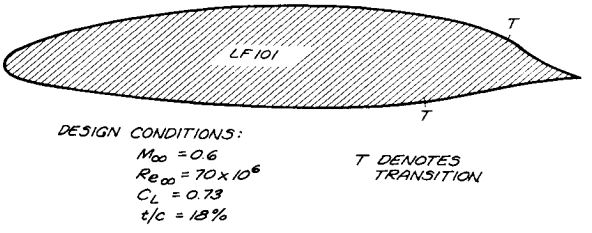

Fig. 21 Airfoil LF101 designed for extensive laminar flow at a high Reynolds number.

The James[7] inverse airfoil design program used in the incompressible airfoil work has the capability for calculating approximate solutions to the subcritical compressible design problem. Figure 18 shows a comparison of the results obtained from the approximate James method with the exact, lifting supercritical case of Nieuwland.[25] Considering that the flow is supercritical, the agreement is remarkably good. The James method will not work for nonisentropic flows where shocks are present.

As an example, airfoil L1003 has been redesigned for $M_\infty = 0.4$ using the James compressible program, and the result is airfoil RP107, shown in Fig. 19. At the design Mach number, the flow is subcritical everywhere. A very interesting result was obtained by analyzing airfoil RP107 using the method of Bauer et al.[26] Figure 19 shows the calculated pressure distributions for Mach numbers of 0.001 (incompressible), 0.475, and 0.500 with the airfoil at its design angle of attack. At $M_\infty = 0.500$, the flow is supercritical over the entire rooftop region, and a shock is located at the beginning of the pressure recovery region. However, at $M_\infty = 0.475$, although the flow is supercritical on the rooftop region, no significant shock is apparent. If a shock exists, it is imbedded in the steep initial gradient of the pressure recovery distribution. The question that comes to mind is, whether or not a shock exists, will the boundary layer survive the steep initial gradient? According to the theoretical method of Cebeci,[21] it will. Additional cases have been studied, including airfoil LR1022M14 shown in Fig. 20. This airfoil was designed for operation at very high altitudes, and hence a fully laminar rooftop at a Reynolds number of 0.5×10^6 was assumed. The pressure distribution shown in Fig. 20 was calculated by the method of Ref. 26 at the design condition of $C_L = 1.0$ at $M = 0.7$, and a wave drag of $C_{D_w} = 0.00035$ was calculated. No separation indicates that a short laminar bubble may occur at the beginning of the pressure recovery region; however, no account has been made for interaction with the weak shock which may exist coincidently with the transition region. It is postulated that said weak shock could

be useful in encouraging or hopefully insuring efficient transition at such low Reynolds numbers. These theoretical results then suggest that a supercritical region can be successfully recovered from using a Stratford-type distribution, and it is possible that this recovery could be nearly isentropic in some cases. It is stressed that this argument is based on relatively limited theoretical results. Further theoretical study is in order, and this should be coupled with an experimental verification.

A third compressible airfoil design is shown in Fig. 21. Airfoil LF101 was designed for extensive laminar flow at high Reynolds numbers. Favorable pressure gradients exist continuously on both surfaces from the leading-edge stagnation point to the transition points indicated in the figure. At a Reynolds number of 70×10^6, the existence of a favorable gradient is not sufficient in itself to maintain laminar flow. The magnitude of the gradient must be greater than a specific value that increases as the local Reynolds number increases. A major difficulty in designing an airfoil with a favorable gradient far aft on both surfaces is that the leading-edge radius tends toward zero, and airfoil LF101 reflects this problem. Theoretical calculations using the method of Cebeci[21] and checking on transition using the Michel-Smith criterion[27] indicate that transition occurs at those points indicated in Fig. 21. This, of course, assumed that the airfoil is perfectly smooth and without waviness. At the design conditions, the flow is subcritical everywhere.

IV. Preliminary Development of Optimized Multielement Airfoils

The design of multielement airfoil systems ordinarily involves the modification of a cruise airfoil in order to provide high lift for takeoff and landing. Extremely rigid constraints relating to mechanical retractability serve to limit the aerodynamicist's freedom in terms of both the shape and orientation of the airfoil elements. The approach to multielement airfoil design to be discussed here is relatively unconstrained when compared with the design problem mentioned previously. In addition to any direct applications of the resulting airfoil designs, it is felt that the basic approach may be useful in guiding the design of a particular element of an otherwise restricted multielement airfoil system. Reference 15 offers a very thorough treatment of the general multielement airfoil theory, and many of the ideas discussed there have been used in the following analysis.

At this writing, the optimized multielement airfoil design problem has not been solved to the extent that the single-element problem has. This is partially a consequence of the lack of an operational inverse airfoil design program for multielement airfoils. The following sections present the basic formulations for the determination of the element chord lengths and pressure distributions, and two hybrid two-element designs that were developed using a combination of the inverse method of Ref. 7 and the direct potential flow calculation method of Ref. 20 are discussed.

A. The Maximum Lift Problem

When considered in a very general form, the problem of maximizing the lift of an airfoil (single- or multielement) in a subcritical flow amounts to attempting to design an airfoil whose $C_p(x)$ distribution fills a "box" in the C_p versus x plane. As shown in Fig. 22, the lower surface of the box is bounded by $C_p=1$, and the upper surface is bounded by $C_p=C_{p_{crit}}$, as implied by the value of the freestream Mach number. This then says that the absolute maximum lift is approximated by $C_L=1-C_{p_{crit}}$, which is not attainable with an unpowered airfoil system. The preceding relation is not exact for compressible flow, since stagnation does not correspond to $C_p=1$. Figure 22 gives a sample comparison between a single-element high-lift airfoil such as L1003 and a two-element airfoil with respect to their ability to fill the box.

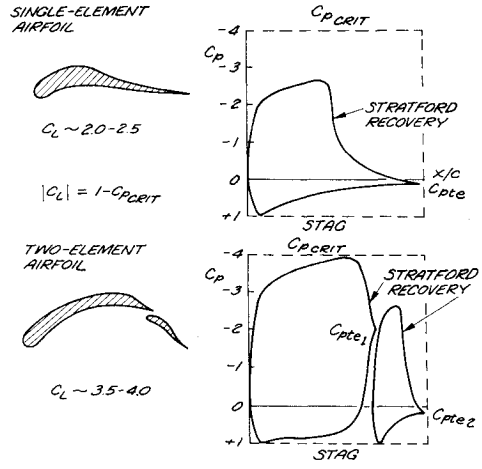

Fig. 22 Definition of maximum lift in the C_p vs x plane.

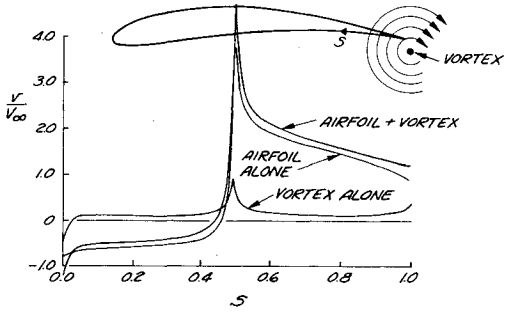

Fig. 23 Point vortex used to represent a flap.

Typically, a multielement airfoil system may be thought of as an exotic combination of a leading-edge slat, main airfoil, and a variety of flap and vane combinations. However, for the unconstrained maximum lift problem, some of these elements may not be necessary. The primary function of a leading-edge slat is to suppress the pressure peak that would otherwise be present at the leading edge of a cruise airfoil when it is operated at a high-lift coefficient. Circulation generated by the slat is used to oppose and hence reduce the velocity of the flow at the leading edge. For the maximum lift problem, the geometry of the main element is not required to be a cruise airfoil, and therefore the leading edge can be shaped to prevent a pressure peak. Consequently, a leading-edge slat will probably not be called for.

B. Two-Element Formulation

To begin, a two-element system is considered where the forward element will be called the main airfoil. Figure 23, from Ref. 28, shows a point vortex located behind an airfoil to simulate a flap, and the increase in the velocity at the trailing edge is apparent. The lift on the airfoil is also increased. The trailing-edge velocity of single-element airfoil is limited to a maximum value of slightly less than unity, as discussed in Sec. II.A. Raising the trailing-edge velocity with a flap will allow the airfoil to carry more lift because the pressure recovery is not required to reach the high pressure level at the trailing edge.

The two-element design problem now becomes one of determining the element chord lengths, pressure distributions, and orientation with respect to one another such that the maximum C_L is obtained. As in the single-element problem, the flow is required to remain unseparated and subcritical everywhere on the airfoil element surfaces, and initially the flow is assumed incompressible. The resulting element geometries should be practical, and they cannot touch each other. Problems associated with boundary-layer interaction can be handled initially by specifying a minimum gap width.

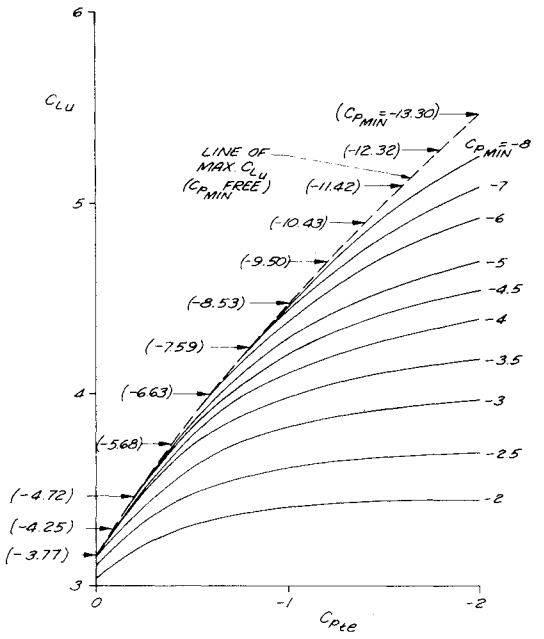

Fig. 24 Upper surface lift as a function of trailing-edge pressure ($C_{pt.e.}$) for fixed rooftop levels (C_{pmin}).

A preliminary estimation of the constraint on relative chord lengths can be obtained from the following argument. Referring to Fig. 22, one might conclude that it is desirable to make the flap chord very small and extend the chord of the main element to take advantage of its load-carrying ability. However, the velocity imposed at the main element trailing edge is proportional to the quantity $(C_L c)_{\text{flap}}$, which implies a lower bound on the flap chord. Also, if the flap chord is too small, the flap Reynolds number will begin to limit the lift coefficient at which it can operate.

The use of a Stratford pressure recovery distribution on the elements of a multielement airfoil is justified by the same argument that was used in the single-element work. Since the flap performance is based on maximizing the quantity $(C_L c)_{\text{flap}}$ (with c being minimized), and the velocity at the trailing edge of the flap must recover to a value slightly less than freestream, a flap velocity distribution similar to that developed for the maximum lift single-element airfoil in Sec. II.C should be appropriate. It is likely that, because of the interaction with the main airfoil, the region of the flap near its leading edge will be shaped differently from the single-element airfoil; however, the remainder of its geometry should be quite similar.

The velocity distribution on the main element is fixed in terms of its rooftop level by the particular value of $C_{p\text{crit}}$ implied by the freestream Mach number, and the upper-surface lift coefficient C_{L_u} of the main element becomes a function of its trailing-edge velocity. As the trailing-edge velocity is increased, the length of the rooftop increases, which, in turn, increases C_{L_u}. Figure 24 shows the effect of trailing-edge pressure ($C_{pt.e.}$) on C_{L_u} for several rooftop levels ($C_{P_{\min}}$). A significant result from this figure is that, for a particular value of $C_{P_{\min}}$, there is a diminishing return for increasing $C_{pt.e.}$ beyond a certain value. For example, at $C_{P_{\min}} = -3$, there is not much to be gained in C_{L_u} beyond $C_{pt.e.} = -1$. Also, $C_{P_{\min}}$ is increased, the "ideal" value of $C_{pt.e.}$ increases. As in the single-element work, it is desired to keep the velocity on the lower surface of the main element as close to stagnation as possible.

Based on the preceding argument, an approximate formulation of the two-element design problem can be offered. For a given Mach number, the main element rooftop level is specified, and a given value for the Reynolds number defines a set of curves similar to those of Fig. 24 from which the ideal value of $C_{pt.e.}$ is determined. This defines an optimized upper-surface velocity distribution for the main element, and the lower-surface distribution is simply set as accelerating and as close to stagnation as possible. The flap velocity distribution is specified similarly to the maximum lift single-element theory.

Up to this point, nothing has been said specifically about the respective element chord lengths. It is suggested that a flap chord on the order of 20% of the total chord would be a good initial choice. (Actually, the choice of chord lengths determines the Reynolds number of each element, which is necessary before their velocity distributions can be defined.)

Next, the velocity distributions are input into an inverse two-element airfoil design program such as James[29] to determine the element shapes and orientation with respect to one another. However, since this program is not operational at this time, the procedure has yet to be carried to completion. It is anticipated that, when the inverse program becomes available, several iterations will be required in order to obtain an acceptable two-segment design. For example, the choice of flap chord length will not be arbitrary. It may be that a 20% flap chord will not provide the ideal of $C_{pt.e.}$ for the main element, or, if it does, the resulting gap between the two elements is too narrow. In principle, the optimum flap chord will be the shortest length that provides the ideal $C_{pt.e.}$ with the minimum acceptable gap.

A potential difficulty concerns the so-called ideal value of $C_{pt.e.}$. Referring to Fig. 24, it can be seen that, if the Mach number is relatively low and hence $C_{p\text{crit}}$ is relatively high, the ideal value of $C_{pt.e.}$ becomes quite high. In this case, it may be that following the approach just described will call for a flap chord that is greater than 50% of the total chord, and it is unlikely that such a solution would provide the maximum lift. The practical upper limit on the flap chord is probably on the order of 25%. This will imply a certain value of $C_{pt.e.}$ on the main element, and the rooftop length should be reduced to meet this value.

Another solution to the problem of the ideal $C_{pt.e.}$ being too high is to use a two-segment flap, and the maximization problem becomes one of considering a three-element system. Until the two-element problem has been thoroughly studied using an exact inverse method to obtain a representative array of complete airfoil designs, it would be impractical to conjecture on the various tradeoffs involved in the three-element problem. It does appear that, as the Mach number is reduced at a fixed Reynolds number, the optimum number of elements will tend to increase. Similarly, as the Reynolds number is increased at a fixed Mach number, the optimum number of elements will also increase.

C. Inverse Multielement Airfoil Design Methods

The previous section stressed the need for an operational inverse method in order for the optimized multielement work to proceed. At least three potential methods are known to exist at this writing. Ormsbee and Chen[9] have approached the problem, and their initial work shows good progress, but it does not appear that their method can be regarded as an operational design tool at this time. Narramore and Beatty[30] have developed and extended the method of Wilkinson[31] with very good results. This requires the airfoil element thickness distributions and the gap and overhang as input, and the method in turn cambers and orients the elements to provide specified pressure distributions on the element upper surfaces. The method is virtually operational, and its utilization is a logical next step in the optimization work. The requirement that the thickness distributions be specified should not prove too restrictive for the initial studies.

It is anticipated that the operational version of James method[29] will be the most versatile of the inverse design techniques for use in the optimization problem. It is the counterpart of the inverse program used in all of the single-element work. As mentioned earlier, conformal mapping

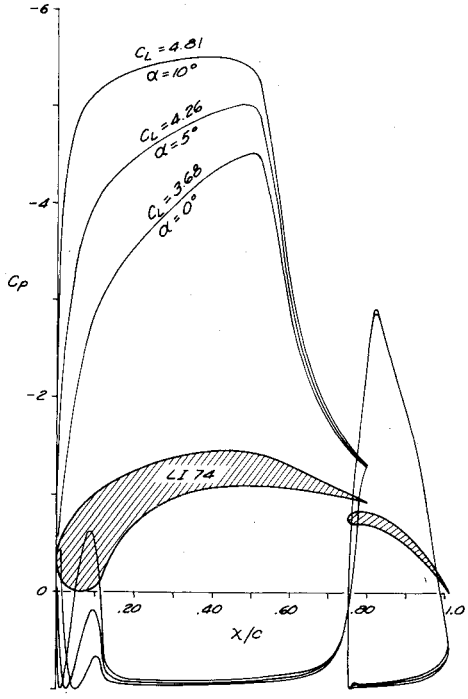

Fig. 25 Airfoil LI74 and its chordwise pressure distributions.

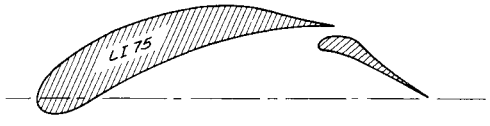

Fig. 26 Airfoil LI75.

theory is employed, and the region between two concentric circles is used as the canonical domain for the doubly connected space defined as the region exterior to the two airfoil elements. The method is capable of providing exact solutions to the three basic problems: direct analysis (both element geometries given), simple design (both element velocity distributions given), and simple mixed (one element geometry and the other element velocity distribution given). This versatility, together with the ability to study the interaction region between the main element and flap in exact detail, makes the James inverse method ideal for the development of the optimum two-element airfoils.

The James method is limited to two-elements; however, most of phenomena of the multielement optimization problem are probably contained in here. Once the two-element problem is understood, the method of Narramore and Beatty, which is, in principle, unlimited as to the number of elements, is available for extension to more than two elements.

D. Example Two-Element Designs

A pair of example two-element high-lift airfoils has been designed by modifying some optimized single-element airfoil geometries and using a cut-and-try approach with the direct solution method of Ref. 20. Their pressure distributions are based on the philosophy discussed in Sec. IV.B, with some concessions made for their particular application, which is discussed in Sec. V. Airfoil LI74, shown in Fig. 25, was designed for maximum possible lift. The main element has a flat rooftop plus Stratford recovery distribution with $C_{pt.e.} \approx -1.0$; however, the flap is a conventional design. (The reason for this is explained in Sec. V.) Figure 26 shows the geometry of airfoil LI75 which was designed for a lower lift coefficient with a higher section L/D as a design goal. Both elements have flat rooftop plus Stratford recovery distributions, and $C_{pt.e.} \approx -1.0$ on the main element. Airfoils LI74 and LI75 were designed for a Reynolds number of 3×10^6 with fully turbulent rooftops.

These airfoils are presented here simply to demonstrate the type of results which should be obtainable from the optimum multielement work. As an aside, it is mentioned that the main element of airfoil LI74 has shown good performance both theoretically and experimentally as a deployed shape for variable-camber-Krüeger leading-edge slat. It provides a very high slat C_L with a relatively low pressure peak because of its long rooftop region.

V. Applications

The application of the airfoil design methods described in this paper to actual design problems is rather limited at this writing. Brief discussions of some of those applications that have received attention are offered below.

A. High-Altitude Long-Endurance Aircraft

The single-element high-lift airfoils appear to have a potential application in high-altitude (>80,000 ft) long-endurance (>24 h) aircraft. Attractive features of the airfoils include high value of the endurance parameter $C_L{}^{3/2}/C_D$ (a consequence of the drag polar maintaining low drag up to $C_{L_{max}}$), very good performance at Reynolds numbers of 10^6 and even below, low values of $C_{mc/4}$ (which can be reduced even further if necessary), and relatively large thickness-to-chord ratios. As a comparison, aft-cambered airfoils tend to suffer at low Reynolds number in terms of increased drag and reduced $C_{L_{max}}$, and such airfoils also offer relatively high values of $C_{mc/4}$ which are not desirable for extremely high-aspect-ratio wings. However, the performance of the airfoils designed by the present method in a compressible flow environment has yet to be verified in a wind tunnel, although the theoretical results discussed in Sec. III.C appear quite promising. Preliminary design studies have very good overall aircraft performance in terms of takeoff gross weight, payload, cruise altitude, and endurance. The airfoils shown in Figs. 13-17 were developed as part of an Air Force Flight Dynamics Laboratory design study for this application.

It should be noted that primary design goal at high altitude is that of maximizing lift, which is proportional to $M^2 C_L$, where M is restricted to remaining subsonic. Airfoil LR1022M14 (shown in Fig. 20) was designed with intent of obtaining an extremum of $M^2 C_L$.

B. Sailplanes

Airfoil L1003M (Figs. 11 and 12) was developed specifically for a high-performance sailplane. One of the design goals was to maximize the endurance parameter $C_L{}^{3/2}/C_D$ which, for a sailplane, equates to minimizing the sinking speed. As discussed in Sec. III, the leading edge was modified to extend the low-drag range to lower lift coefficients, and this, coupled with the negative deflection of the flap, should provide good high-speed performance. A sailplane using airfoil L1003 has been designed with a wing span of 60 ft and a 20-in. chord. Each of the two wing panels is to be extruded from a single piece of aluminum.

C. Propellers, Fans, and Windmills

Very preliminary calculations have indicated that the high-lift airfoils should provide significant performance improvements for propellers of general-aviation-type aircraft. The performance comparison given in Table 1 was made by AeroVironment, Inc., of Pasadena, Calif., using standard blade element theory assuming uniform induced axial flow, no swivel component, and a constant chord blade at uniform lift coefficient. The "standard" propeller has a Clark Y airfoil, and the modified propellers use airfoil L1003M, and the performance is based on a 150-hp light airplane taking off at 52 knots.

Table 1 Performance comparison

	Thrust, lb	Diameter, ft	rpm	dB
Standard propeller	550	6.0	2870	98
Modified propeller I	650	6.0	1300	92
Modified propeller II	580	6.0	2870	93

Table 2 Test results

	Commercial fan	Payne Engineering fan
Diameter	30 in.	30 in.
Number of blades	12	6
Rpm	2500	2500
Input hp	40	40
Normalized thrust	1.0	1.15
dBA at 50 ft	105	85

The comparison is impressive; however, it is stressed that these are approximate calculations. Airfoil L1003M was not designed with the propeller application in mind, and a serious effort in this area should begin with the development of an airfoil specifically for propellers. From a general point of view, the following advantages appear: increased efficiency, reduced tip speed, reduced number of blades, and reduced noise level.

A similar potential application lies in the area of high-thrust fans. Henry Payne of the Payne Engineering Company of Scott Depot, W. Va., has designed a prototype ducted fan using an airfoil similar to L1003 which is shown in Fig. 27. This fan was compared with a "conventional," fan which used circular arc airfoil sections, and the test results are shown in Table 2.

Payne has also tested a seven-blade version of this fan, and it was capable of absorbing 50 hp at 2500 rpm. These results appear to be promising; however, like the propeller work, more development and testing are in order. This should include the development of airfoil sections for a fan application where cascade effects are considered.

The windmill application also appears to be natural for airfoils such as L1004, or possibly LA2566. Windmills typically operate at blade lift coefficients of 1.0 and above, and conventional airfoils have relatively high profile drag, particularly at low Reynolds numbers. Calculations based on airfoil L1003 show improved efficiency in terms of power available at all wind speeds. Also, the relatively low pitching moment is appealing from a structural point of view.

D. Wings for Racing Cars and the Concept of the Gurney Flap

The wings on race cars are inverted and used to provide "downforce" as opposed to lift, and this downforce acts to increase the adhesion of the tires during acceleration, braking, and, most importantly, in cornering. An appreciation for the performance increment offered by the wings can be obtained from a comparison of pole position qualifying speeds at Indianapolis, where in 1970 with no wings the speed was 172 mph, and 1972 with relatively crude wings it was 196 mph. At the latter lap speed, the lateral force in the turns is on the order of 2.3 g. The wings are located on the nose of the car and behind the rear wheels, as shown in Fig. 28.

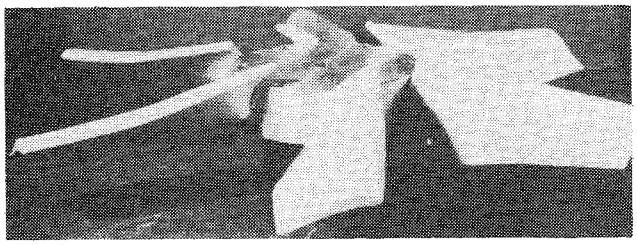

Fig. 27 Axial flow fan designed by Payne Engineering of Scott Depot, W. Va.

Airfoil L174 (Fig. 25) was designed with maximum possible C_L in mind. The two-dimensional pressure distribution was specified with the consideration that the very low aspect ratio would serve to reduce the rooftop level to a more conservative value. The flap geometry was specified by existing hardware, and its orientation was set to obtain the highest possible $C_{pt.e.}$ on the main element. This airfoil worked quite well on the race car in terms of providing the required downforce, and yarn tufts showed that the flow was completely attached on both elements. The flap required the addition of a "Gurney flap" (to be described shortly) in order to remain attached. Airfoil LI74 did, however, have some undesirable characteristics: it tended to separate in crosswinds (a consequence of the car drifting to a large yaw angle in a turn), and its unseparated angle-of-attack range was quite small (approximately 5 deg).

The Gurney flap mentioned previously is simply a flat plate on the order of 1% of the chord length which is located perpendicular to the pressure side of the airfoil at the trailing edge (see Fig. 29). Race car testing by Gurney has indicated that his device increases the downforce and reduces the drag as measured by a comparison of corner and straightaway speeds with and without the flap. Increasing the Gurney flap chord beyond approximately 2%, while continuing to increase the downforce, also begins to increase the drag noticeably.

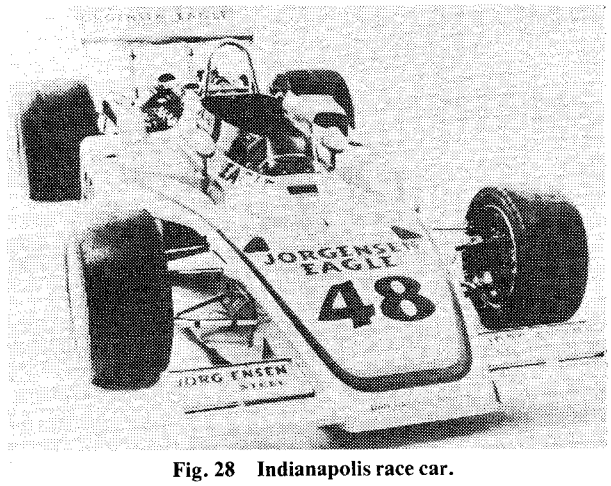

Fig. 28 Indianapolis race car.

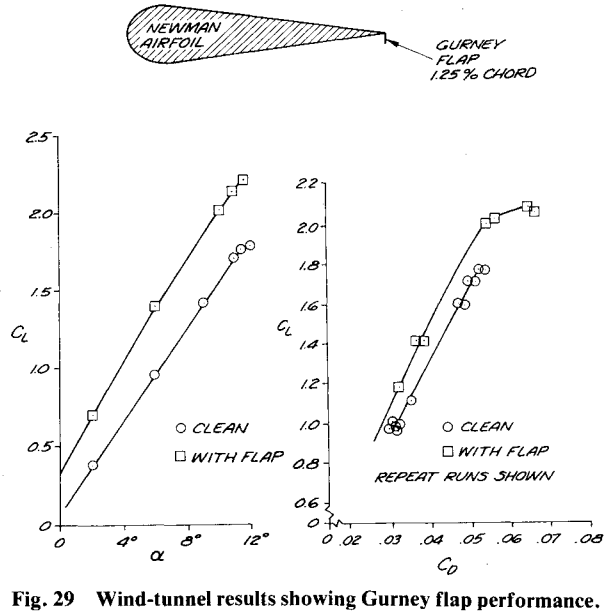

Fig. 29 Wind-tunnel results showing Gurney flap performance.

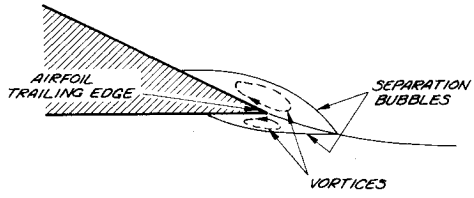

Fig. 30 Trailing-edge flow conditions of a conventional airfoil at a moderate lift coefficient.[32]

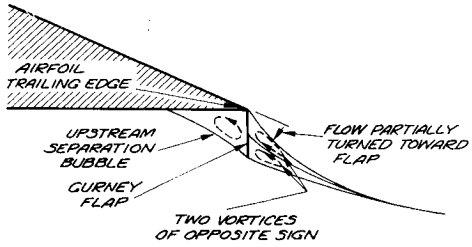

Fig. 31 Hypothesized trailing-edge flow conditions of the airfoil of Fig. 30 with a Gurney flap.

A wind-tunnel test of the Gurney flap was conducted in the Douglas Long Beach low-speed wind-tunnel, and a typical result is shown in Fig. 29. (The Newman airfoil is defined by an elliptical nose on a straight-line wedge. It is a canonical form used to check boundary-layer theories, and it provides a long adverse gradient region.) These results indicate that the drag is reduced and the lift is increased. It was expected that the Gurney flap would provide increased lift at a given angle of attack and a higher value of $C_{L_{max}}$; however, the fact that the drag at a given lift coefficient was apparently reduced needs explanation.

The specific details of the flow mechanism at the trailing edge of a conventional airfoil are not completely understood at this time. Kuchemann[32] discusses the flow near the trailing edge, and he shows that Prandtl's boundary-layer theory cannot be applied there. This a consequence of the assumption no longer being valid that the component of velocity normal to the airfoil surface is negligibly small. He also shows that near the trailing edge of an airfoil a local separation bubble is quite likely, particularly for airfoils with larger trailing-edge angles.

In relation to the apparent drag reduction obtained with the Gurney flap, the flow pictures in Figs. 30 and 31 are considered. Figure 30 shows the flow near the trailing edge of a conventional airfoil operating at a moderate lift coefficient with separation bubbles similar to those proposed by Kuchemann for the nonlifting case. Figure 31 is a hypothesis of the flow conditions about the Gurney flap. During the wind-tunnel test, a tufted probe indicated that there was a significant turning of the flow over the back side of the flap, as shown in Fig. 31. The tuft also indicated a reverse flow region behind the flap which is modeled by the two vortices shown in the figure.

It is possible that the wake momentum deficits for the two flows depicted in Figs. 30 and 31 are of the same level, and the deficit produced by the Gurney flap could be slightly lower, depending on the airfoil trailing-edge angle and the size of the flap. Consequently, it is felt that the drag results of Fig. 29 are not implausible, particularly in the case of thick airfoils. Further testing to obtain verification is, of course, in order. However, the results obtained thus far indicate that one of the virtues and applications of the Gurney flap may be as a drag-reducing as well as lift-increasing device on both single- and multielement airfoil systems. This concept has also been considered by other investigators, such as Duddy.[33]

Airfoil LI75 was designed at a lower lift coefficent for improved L/D. The rooftop level of the main element is substantially lower, and the flap is a modification of airfoil L1004. A Gurney flap is not required for the flow to remain attached on the flap, although in some instances it has been used to increase the downforce in lieu of increasing the airfoil angle of attack. This airfoil has a low-drag angle-of-attack range of approximately 8 deg and has not demonstrated any sensitivity to crosswinds. It was used on the race car that won the 1975 Indianapolis 500 Mile Race.

The foregoing discussion provides a good point on which to close this paper. Of the various potential applications for modern airfoil technology, racing car wings would probably not rank highly in the mind of the aerodynamicist. Curiously, this particular application has offered the opportunity to proceed directly from theory, concept, and design to fabrication, test, and operation, in an extremely short time span. It is felt that the results demonstrate the capability of the airfoil design methods described in this paper to be applied to a highly constrained problem, with success in this particular case. Hopefully, similar successes will be found in more conventional aerodynamic applications.

Acknowledgment

The airfoil designs and their development described in this paper are a product of 10 years of study at the Douglas Aircraft Company of the McDonnell Douglas Corporation, and are covered by a pending McDonnell Douglas patent. A substantial portion of the work was conducted under the Douglas Independent Research and Development program. In addition, some recent applications of the design methods have been supported by contracts from the U.S. Government, including the Air Force Flight Dynamics Laboratory. Information, ideas, and suggestions have been supplied by many individuals throughtout the past decade. The following is a partial list of those who have provided important technical contributions: J. G. Callaghan, T. Cebeci, D. S. Gurney, R. M. James, K. Kaups, P. B. S. Lissaman, A. I. Ormsbee, A. E. Sewell, A. M. O. Smith, D. N. Smyth, and G. O. Wheeler.

References

[1] Lighthill, M. J., "A New Method of Two-Dimensional Aerodynamic Design," Aeronautical Research Council, London, R&M 2112, 1945.

[2] Wortmann, F. X., "Ein Beitrag zum Entwurf von Laminarprofilen für Segelflugzeuge und Hubschrauber," *A. Flugwiss,* Vol. 3, 1955.

[3] Goldstein, A. W. and Mager, A., "Attainable Circulation of Airfoils in Cascade," NACA TN 1941, 1949.

[4] Liebeck, R. H., "Optimization of Airfoils for Maximum Lift," Ph.D. Thesis, Univ. of Illinois, Urbana, Ill., 1968; also Liebeck, R. H. and Ormsbee, A. I., "Optimization of Airfoils for Maximum Lift," *Journal of Aircraft*, Vol. 7, Sept-Oct. 1970, pp. 409-415.

[5] Weber, J., "The Calculation of the Pressure Distribution on the Surface of Thick Cambered Wings and the Design of Wings with Given Pressure Distribution," Aeronautical Research Council, London, R&M 3026, 1955.

[6] Liebeck, R. H. and Smith, A. M. O., "A Class of Airfoils Designed for High Lift without Separation in Incompressible Flow," Douglas Aircraft Co., Long Beach, Calif., Rept. MDC J1097/01, (restricted distribution); also Liebeck, R. H., "A Class of Airfoils Designed for High Lift in Incompressible Flow," *Journal of Aircraft*, Vol. 10, Oct. 1973, pp. 610-617.

[7] James, R.M., "A New Look at Two-Dimensional Incompressible Airfoil Theory," Douglas Aircraft Co., Long Beach, Calif., Rept. MDC J0918/01, 1971 (restricted distribution).

[8] Liebeck, R.H., "Wind Tunnel Tests of Two Airfoils Designed for High Lift without Separation in Incompressible Flow," Douglas Aircraft Co., Long Beach, Calif., Rept. MDC J5667/01, 1972 (restricted distribution).

[9] Ormsbee, A.I. and Chen, A.W., "Multiple Element Airfoils Optimized for Maximum Lift Coefficient," *AIAA Journal*, Vol. 10, Dec. 1972, pp. 1620-1624.

[10] Sivier, K.R., Ormsbee, A.I., and Awker, R.W., "Low Speed Aerodynamic Characteristics of a 13.1 Percent-Thick, High-Lift Airfoil," Society of Automotive Engineers, Paper 740366, April 1974.

[11] Pick, G.S. and Lien, D.A., "The Development of a Two-Dimensional High-Endurance Airfoil with Given Thickness Distribution and Reynolds Number," Naval Ship Research and Development Center, Bethesda, Md., Sept. 1972.

[12] Strand, T., "Exact Method of Designing Airfoils with Given Velocity Distribution in Incompressible Flow," *Journal of Aircraft*, Vol. 10, Nov. 1973, pp. 651-659.

[13] Arlinger, G., "An Exact Method of Two-Dimensional Airfoil Design," SAAB, Linköping, Sweden, TN 67, Oct. 1970.

[14] Wortmann, F.X., "The Quest for High Lift," AIAA Paper 74-1018, Sept. 1974.

[15] Smith, A.M.O., "High-Lift Aerodynamics," *Journal of Aircraft*, Vol. 12, June 1975, pp. 501-530.

[16] Stratford, B.S., "The Prediction of Separation of the Turbulent Boundary Layer," *Journal of Fluid Mechanics*, Vol. 5, 1959, pp. 1-16.

[17] Stratford B.S., "An Experimental Flow with Zero Skin Friction Throughout Its Region of Pressure Rise," *Journal of Fluid Mechanics*, Vol. 5, 1959, pp. 17-35.

[18] Liebeck, R.H., "A Class of Airfoils Designed for Reynolds Numbers of Less than 0.50×10^6," Douglas Aircraft Co., Long Beach, Calif., Rept. MDC J7220/01, 1976 (restricted distribution).

[19] Callaghan, J.G. and Beatty, T.D., "A Theoretical Method for the Design and Analysis of Multi-Element Airfoils," *Journal of Aircraft*, Vol. 9, Dec. 1972, pp. 844-848.

[20] Hess, J.L. and Smith, A.M.O., "Calculation of Potential Flow about Arbitrary Bodies," *Progress in Aeronautical Sciences*, edited by D. Kuchemann, Vol. 8, Pergamon Press, New York, 1966.

[21] Cebeci, T., Smith, A.M.O., and Wang, L.C., "A Finite-Difference Method for Calculating Compressible Laminar and Turbulent Boundary Layers," Douglas Aircraft Co., Long Beach, Calif., Rept. DAC 67131, 1969.

[22] Lee, D.G. and Lacey, D.W., "Wind Tunnel Results of a Ten-Percent Scale Powered SCAT VTOL Aircraft," Naval Ship Research and Development Center, March 1977.

[23] Cebeci, T., "On the Solution of Local Nonsimilar Boundary-Layer Equations for Standard and Inverse Flows," *Letter in Heat and Mass Transfer*, Vol. 2, Pergamon Press, New York, 1975.

[24] Liebeck, R.H., "Superlift Airfoil Development Program," Air Force Flight Dynamics Lab., AFFDL-TR-75-110, Oct. 1975.

[25] Nieuwland, G.Y., "Transonic Potential Flow Around a Family of Quasi-Elliptical Airfoil Sections," N.L.R., Rept. TR T172, 1967.

[26] Bauer, F., Garabedian, P., and Korn, D., *Supercritical Wing Sections*, Springer-Verlag, New York, 1972.

[27] Smith, A.M.O. and Gamberoni, N., "Transition, Pressure Gradient, and Stability Theory," Douglas Aircraft Co., Long Beach, Calif., Rept. ES 26388, August. 1956.

[28] Liebeck, R.H. and Smyth, D. N., "Study of Slat-Airfoil Combinations Using Computer Graphics," *Journal of Aircraft*, Vol. 10, April 1973, pp. 254-256.

[29] James, R.M., "Analytical Studies of Two-Element Airfoil Systems," Douglas Aicraft Co., Long Beach, Calif., Rept. MDC J6850/01, 1975.

[30] Beatty, T.D., and Narramore, J.C., "An Inverse Method for Design of Multi-Element High-Lift Systems," *Journal of Aircraft*, Vol. 13, June 1976, pp. 393-398.

[31] Wilkinson, D.H., "A Numerical Solution of the Analysis and-Design Problems for the Flow Past One or More Aerofoils on Cascades," Aeronautical Research Council, R&M 3545, 1967.

[32] Kuchemann, D., "Inviscid Shear Flow Near the Trailing Edge of an Airfoil," *A. Flugwiss*, Vol 15, 1967.

[33] Duddy, R.R., "High Lift Devices and Their Uses," 778th Lecture to the Royal Aeronautical Society, April 1949.